# Imaging findings in hippocampal sclerosis: correlation with pathology.

R A Bronen, G Cheung, J T Charles, J H Kim, D D Spencer, S S Spencer, G Sze and G McCarthy

*AJNR Am J Neuroradiol* 1991, 12 (5) 933-940
http://www.ajnr.org/content/12/5/933

# Imaging Findings in Hippocampal Sclerosis: Correlation with Pathology

Richard A. Bronen[1]
Gordon Cheung[1,2]
Joseph T. Charles[1,3]
Jung H. Kim[4]
Dennis D. Spencer[5]
Susan S. Spencer[6]
Gordon Sze[1]
Gregory McCarthy[5]

**We evaluated the ability of preoperative radiologic imaging to detect hippocampal sclerosis in 31 patients who underwent surgery for intractable epilepsy. Hippocampal sclerosis is commonly associated with surgically treatable temporal lobe epilepsy. It is pathologically described as neuronal cell loss with associated gliosis in the hippocampus. While previous reports have correlated imaging results with clinical or qualitative histologic findings, this study used quantitative pathologic criteria (neuronal cell density) to diagnosis hippocampal sclerosis. We focused our study on the 11 patients with cryptogenic temporal lobe epilepsy. Of these, nine had hippocampal sclerosis by pathologic criteria. MR findings included unilateral hippocampal atrophy, an increased signal in the hippocampus on long TR scans, and atrophy in the adjacent white matter and temporal lobe. Hippocampal atrophy was most frequently seen in the red nucleus plane on coronal scans, corresponding to the body of the hippocampus. We also compared hippocampal size on MR with neuronal density in surgical specimens of the 11 patients with cryptogenic temporal lobe epilepsy. A statistically significant correlation was found between MR size and neuronal density in CA3 and CA4 of the cornu ammonis and the granular cell layer of the hippocampus.**

**Since temporal lobectomy eliminated seizures in seven of nine patients with hippocampal sclerosis, preoperative diagnosis by MR has important therapeutic consequences.**

***AJNR* 12:933–940, September/October 1991**

Received July 12, 1990; revision requested October 4, 1990; revision received February 19, 1991; accepted February 27, 1991

Presented at the annual meeting of the American Society of Neuroradiology, Orlando, FL, March 1989.

[1] Department of Diagnostic Imaging, Yale University School of Medicine, 333 Cedar St., New Haven, CT 06510. Address reprint requests to R. A. Bronen.

[2] Present address: Department of Diagnostic Radiology, Sunnybrook Health Science Centre, University of Toronto, 2075 Bayview Ave., North York, Ontario M4N 3M5, Canada.

[3] Present address: Radiology Imaging Associates, 2306 Nebraska Ave., Fort Pierce, FL 34950.

[4] Section of Neuropathology, Yale University School of Medicine, New Haven, CT 06510.

[5] Section of Neurosurgery, Yale University School of Medicine, New Haven, CT 06510.

[6] Department of Neurology, Yale University School of Medicine, New Haven, CT 06510.

0195–6108/91/1205–0933


Hippocampal sclerosis (HS), also known as Ammon's horn sclerosis or mesial temporal sclerosis, is the most common disorder associated with medically intractable temporal lobe epilepsy (TLE) [1–8]. HS describes an entity of neuronal cell loss with associated gliosis involving the hippocampal formation (which we refer to as the hippocampus). Medically refractory chronic TLE often can be treated by surgical resection. Temporal lobectomy in patients with HS is associated with a very good outcome [9, 10]. Preoperative diagnosis of HS therefore would be important for the successful surgical treatment of chronic, uncontrolled TLE.

As part of a comprehensive protocol, we routinely evaluate medically uncontrolled epilepsy patients diagnostically by MR imaging, CT, angiography, and electroencephalography (EEG) [11]. In this study, we assessed the imaging characteristics of the hippocampus, temporal horn, and temporal lobe in 31 patients with intractable epilepsy who subsequently underwent surgery, and correlated the imaging findings with EEG and pathologic findings. Since the criteria for HS have been somewhat ambiguous, we decided to use hippocampal neuronal density, a reproducible quantitative value, to determine which patients with TLE had HS. Most previous MR studies have relied on clinical or qualitative histologic criteria [12–18].

The first phase of the study consisted of blinded evaluations of the MR and CT scans. In the second phase, we reevaluated the MR scans of those 11 patients who underwent temporal lobectomy for possible HS (cryptogenic TLE) to look for similarities that might have been missed in the blinded evaluation. The third phase

addressed whether hippocampal size on MR is related to neuronal density in patients with cryptogenic TLE, since surgical benefit appears related to neuronal loss; that is, elimination of seizures by temporal lobectomy occurs in up to 90% of patients when there is severe depletion of neurons as opposed to nonspecific gliosis or minimal neuronal loss [19–22]. We chose to develop simple criteria for assessing hippocampal size that can be applied during routine clinical practice. In a separate group of patients, a recent quantitative study showed a positive correlation between MR appearance and cell counts [23]. Currently, volumetric studies are not widely available since they are labor intensive and require specialized programs.

## Materials and Methods

### *Patient Population*

We retrospectively studied 31 patients with medically intractable complex partial epilepsy who were treated surgically (temporal lobectomy, lesion excision, or callosotomy) between 1986 and 1988. The patients ranged in age from 15 to 47 years and had had epilepsy for 3–39 years. This report's main focus is on the 11 TLE patients without a macroscopic structural lesion (i.e., cryptogenic TLE) who underwent temporal lobectomy and had quantitative hippocampal cell counts.

### *Diagnostic Studies*

MR scans were obtained on a 1.5-T magnet (General Electric, Milwaukee, WI) with T1-weighted sequences in the sagittal plane and proton-density– and T2-weighted sequences in the axial and coronal planes. Parameters for the T2-weighted scans included 2000–3000/60–100/1 (TR/TE/excitations), 20- to 24-cm field of view (FOV), and 5-mm-thick slices with a gap of 2.5 mm. Additional T1-weighted coronal sequences consisted of 400/20/4, 5-mm contiguous slices, and 16-cm FOV. CT scans were obtained without and with IV contrast material on GE 8800 and 9800 CT scanners. In concert with the intracarotid Amytal (Wada) study, angiography of the internal carotid artery systems was performed. When history, cognitive testing, scalp EEG/audiovisual seizure monitoring, and imaging studies were not concordant, invasive monitoring with depth and/or subdural electrodes was obtained.

### *Phase 1*

In the first phase of this study, MR scans from the 31 patients were evaluated independently by two neuroradiologists who were blinded with respect to clinical history, EEG, CT, MR, surgical site, and pathology. CT scans were interpreted in a similar fashion 6 weeks later. Interpretations of angiographic, EEG, and clinical data were obtained in a nonblinded fashion.

The left and right hippocampal formations, temporal horns, and temporal lobes were evaluated for asymmetry of size. Grading criteria consisted of (1) definite asymmetry, (2) subtle or questionable asymmetry, and (3) no asymmetry. Hippocampal signal intensity was studied also. Focal abnormalities (macroscopic foreign tissue lesions such as tumors, vascular malformations, or hamartomas) were catalogued and are the subject of another article. Patient head rotation was determined by assessing symmetry of the internal auditory canal [24].

A retrospective study that included only patients with HS would certainly have biased our interpretation of hippocampal symmetry. Owing to the special sequence we used to evaluate epileptic patients (i.e., small-FOV coronal T2-weighted examinations prior to axial studies), we could not use nonepileptic MR examinations (such as of patients with headaches) as controls for the blinded portion of this study. As a form of control, we included epileptic patients who were treated with surgery. These patients included those with macroscopic lesions, those who underwent corpus callosotomy, and those who underwent temporal lobectomy but were found to have relatively normal histology.

### *Phase 2*

The second phase of this study involved reevaluation of MR scans after pathologic results were known. We specifically reviewed studies of those 11 patients who underwent temporal lobectomy for cryptogenic TLE. MR findings of hippocampal atrophy were determined by consensus agreement by two neuroradiologists. Findings not initially evaluated in phase 1 (i.e., collateral white matter atrophy and hippocampal shape) were evaluated in phase 2. We assessed the thickness of the white matter located between the hippocampus and collateral sulcus, which we referred to as the collateral white matter (Fig. 1).

In this second phase, we also evaluated which region of medial temporal gray matter was affected by HS. Abnormal hyperintensity on T2-weighted images and gray matter atrophy were assessed. We divided the medial temporal gray matter into 10 segments 5 mm thick based on anatomic landmarks found on coronal MR: anterior pituitary, posterior pituitary, suprasellar cistern, basilar artery, interpeduncular cistern, red nucleus, posterior to the red nucleus, superior colliculus, inferior colliculus, and posterior to the colliculi. Besides determining which coronal plane was being affected, we also determined which of four segments of medial temporal gray matter was affected by HS: the amygdala or hippocampal head (pes), body, or tail.

### *Phase 3*

In this phase, we compared the size of the hippocampus on MR with neuronal density in the cryptogenic TLE group ($n$ = 11). We evaluated the hippocampus in the coronal plane at the level of the red nucleus. We chose this plane in order to evaluate the hippocampus at its body at an easily recognizable landmark. Because of the complex configurations of the head (pes) and tail, we thought the most reproducible results would be obtained by evaluating the hip-

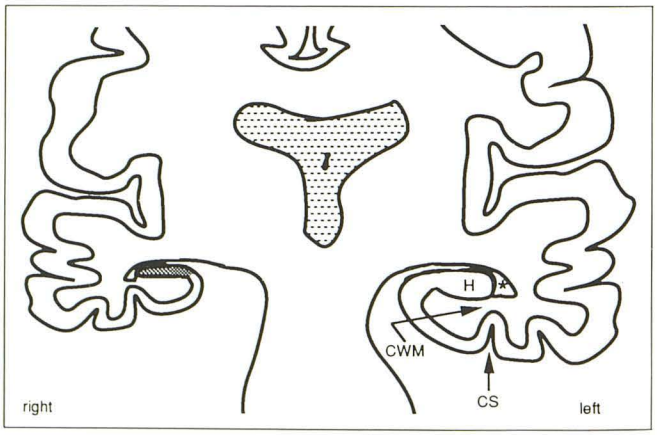


**Fig. 1.—Diagrammatic representation of idealized right hippocampal sclerosis on a coronal MR slice. Right hippocampus is atrophic and hyperintense (*shaded area*). Ipsilateral temporal lobe and collateral white matter are asymmetrically small. Although adjacent temporal horn dilatation can be a secondary sign of hippocampal sclerosis, anterior asymmetry of temporal horn can occur often enough in normal persons to invalidate this as a primary sign (as illustrated in this case). On left side, H = hippocampus, *asterisk* = temporal horn, CWM = collateral white matter, CS = collateral sulcus.**

pocampal body. A second reason to study the hippocampus at its body is that the cell counts by our pathologists were performed in the body, again for reasons of consistency and reproducibility [25].

We measured the craniocaudal (height) and transverse (width) dimensions of the hippocampus, and calculated the product of height × width. We also examined the ratio of the surgical to nonsurgical side for these measurements. Since the height or vertical dimension of the hippocampus on coronal sections is influenced by the degree of head extension, we used a correction factor for height. As with a cylinder, the shortest dimension and most consistent results can be obtained if one uses cross sections that are perpendicular to the long axis of the hippocampus. Thus, we corrected all height measurements to a 90° hippocampal angle. Hippocampal angle, measured on parasagittal T1-weighted studies, was defined as the angle formed by the plane of the coronal slices and a plane parallel to the inferior aspect of the left hippocampal formation (the cornu ammonis and subiculum) at the region of the body (Fig. 2). Hippocampal angle ranged from 55° to 88° with an average of 70°. The following formula was used to correct the height to 90°:

$$\text{Corrected height} = \text{raw height} \times \sin \theta,$$

where $\theta$ equals the hippocampal angle [26].

We compared MR measurements of the hippocampus at the level of the red nucleus—height; width; product (height × width); and ratio (surgical/nonsurgical side) of height, width, and product—with neuronal densities of the cornu ammonis fields (CA1–CA4) and the dentate granular layer. Statistical analysis used the Pearson product-moment correlation coefficient.

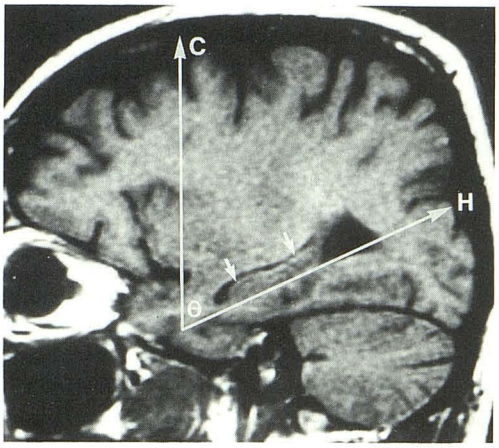


**Fig. 2.—Hippocampal angle on a parasaggital T1-weighted MR image. Hippocampal angle ($\theta$) is formed by interception of plane of coronal MR slice (*line C*) with plane (*line H*) parallel to inferior aspect of hippocampal formation (*arrows*).**

### *Surgery and Pathology*

All cryptogenic TLE patients underwent anteromedial temporal lobectomy and radical hippocampectomy as described previously by Spencer et al. [11, 27]. The hippocampus was always removed en bloc from the temporal lobe. Cell counting was performed on 6-$\mu$m coronal paraffin sections at the level of the hippocampal body. The specimens were stained with either Nissl or hematoxylin and eosin. The count was repeated on five consecutive histologic sections by two investigators without knowledge of clinical history of individual cases [25]. Neuronal density was expressed as the mean number of neuronal cells per cubic millimeter for each hippocampal subdivision, the cornu ammonis fields (CA1–CA4) and the dentate granular layer (Fig. 3).

### *Criteria for HS*

Kim et al. [25] found neuronal density in the hippocampus in HS to be 35–50% that of controls. We defined HS for purposes of this preliminary study as greater than 50% loss of neuronal density compared with controls in either the average of the pyramidal cells of the cornu ammonis fields or the granular cells of the dentate gyrus [25].

## Results

Pathologic findings are found in Table 1. Clinical and imaging results for the 11 patients with cryptogenic TLE are


**Fig. 3.—*A*, Diagrammatic representation of a coronal slice through level of red nucleus. Area of left hippocampus enclosed in box identifies region of interest in *B* and *C*.**

***B*, Normal coronal histologic specimen. Normal pyramidal cells in cornu ammonis (Ammon's horn) form a band of dark particles. On the basis of cytoarchitecture, cornu ammonis (CA) can be segmented into four regions, CA1–CA4 fields. Granule cells in dentate gyrus (D) form a thinner and darker U-shaped band around CA4. (Nissl stain, original magnification × 16.3)**

***C*, Histologic specimen of hippocampal sclerosis shows almost complete loss of pyramidal cell layer in CA1, as noted by absence of band of dark particles seen in *B*. There is marked cellular depletion in remainder of cornu ammonis and dentate gyrus, resulting in atrophy of hippocampus as a whole. Neuronal density of each region was determined by means described in text. (Nissl stain, original magnification × 18.1)**

**TABLE 1: Pathologic Findings in Patients Who Had Surgery for Intractable Epilepsy**

| Finding | No. of Patients |
|---|---|
| Hippocampal sclerosis | 9 |
| Gliosis | 2 |
| Glioma | 13 |
| Vascular malformation | 2 |
| Nonspecific calcification | 1 |
| Hamartoma | 1 |
| Gliomesenchymal scar | 1 |
| Callosotomy | 2 |

Note.—Hippocampal sclerosis was regarded as greater than 50% hippocampal neuronal loss; gliosis was regarded as less than 50% hippocampal neuronal loss.

shown in Table 2. Hippocampal atrophy and signal abnormality on MR helped identify patients with HS (Figs. 4–6). In no case was hippocampal atrophy observed on the side opposite pathologically proved HS. The blinded MR interpretations by two observers resulted in correctly identifying five of nine and six of nine patients with HS. The nonblinded evaluation (phase 2) found unilateral hippocampal atrophy in eight of the nine HS patients. Table 3 charts regional hippocampal atrophy. The normal oval shape of the hippocampus on coronal slices (at the red nucleus plane) becomes triangular or flattened in these patients. Hippocampal signal was hyperintense on long TR sequences. Hyperintensity was always confined to the hippocampal gray matter; that is, abnormal signal in adjacent white matter was never seen in our patient population. The proton-density sequence was used to differentiate abnormal hippocampal signal from CSF in the temporal horn or choroidal fissure.

The results from phase 3, the Pearson product-moment correlation analysis comparing MR measurements with cell density, are shown in Table 4. The strongest correlations occurred between the MR product and neuronal densities in CA3 ($r = .7645$, $p < .03$), CA4 ($r = .6698$, $p < .03$), and the dentate gyrus ($r = .6882$, $p < .02$).

Of the remaining 20 patients, five had asymmetrically small hippocampi. Four of these had adjacent temporal lobe lesions. The fifth underwent callosotomy for bilateral seizure foci.

Temporal lobe asymmetry (resulting in a smaller left side) occurs normally [23, 24, 28]. There was asymmetry in temporal lobe size in 23 of the 31 patients (the left side was smaller in 18, the right in five). Those with a smaller right side consisted of two patients with tumors and three with right HS. Right speech dominance occurred in only two patients, both with left-sided structural lesions and a symmetric or smaller left temporal lobe.

Temporal horn asymmetry was seen in half the HS patients, usually with enlargement occurring on the ipsilateral side (Table 2). In the 20 patients not described in Table 2, asymmetry was noted in seven patients: five with gliomas, one with a vascular malformation, and one with a callosotomy.

Coronal T2-weighted images in conjunction with contiguously sliced coronal T1-weighted images with a small FOV were optimal for evaluating HS. Hippocampal size and signal intensity, temporal lobe, temporal horn, and collateral white matter could all be assessed.

## Discussion

Recent neuroanatomic investigations have helped define the abnormalities expressed clinically as TLE. In patients with medically intractable TLE, MR imaging can separate those with cryptogenic TLE who may have HS from those with lesions (lesional TLE) [12–14]. Several reports [22, 25, 29, 30] now suggest these two groups can be separated not only on the basis of qualitative histology, but also by clinical history, EEG findings, hippocampal neuronal cell counts, and immunohistochemical analysis. Cryptogenic TLE itself appears to be composed of two groups that can be separated by a similar set of parameters and most importantly, postoperative prognosis: (1) typical cryptogenic TLE, or HS, and (2) atypical cryptogenic TLE, which represented 14% of cryptogenic TLE cases in a recent article [22].

In the HS group, there is (1) marked neuronal depletion in the range of 35–50% compared with controls in the cornu ammonis fields and dentate gyrus, (2) selective loss of somatostatin and neuropeptide Y immunoreactive interneurons, (3) selective axonal sprouting in the dentate region, (4) often a history of febrile seizures, (5) localization of the seizure focus to the medial temporal lobe, and (6) cure or elimination of greater than 90% seizures with temporal lobectomy [22, 25, 29, 30]. HS is the most common abnormality associated with medically refractory TLE, occurring in 47–85% of cases [1–8].

The atypical cryptogenic TLE patients differ significantly from the HS group. Many features including cell numbers, interneuron distribution, and axonal sprouting resemble those of the lesional TLE and nonepileptic control groups. These patients have mild gliosis without the accompanying severe neuronal loss in the hippocampus. Compared with the hippocampal sclerosis group, the epileptogenic focus is not as well localized to the medial temporal lobe and the surgical outcome is much poorer [19–22].

Conflicting or poorly characterized imaging results have been reported in HS. A major obstacle to the interpretation of these studies has been the definition of the entity itself. Few imaging studies clearly state their pathologic criteria, and even fewer relate imaging findings to a quantified value of hippocampal neuronal loss. We tried to address this problem by using quantified criteria (i.e., greater than 50% neuronal loss) for our definition of HS [25].

Until recently, hippocampal atrophy has been reported infrequently. In four MR studies with a total of 85 patients with surgically proved "hippocampal sclerosis," there was no mention of hippocampal atrophy [13–16]. MR studies of TLE that used visual assessment have noted hippocampal atrophy in one of 31 [17] and 28 of 41 [18] patients. Unilateral hippocampal atrophy was found in eight of our nine patients. The hippocampus lost its normal oval configuration and often became flat. The findings often were subtle, and this resulted in interobserver differences. However, in phase 1 we were on a learning curve. With increasing experience, we became more attuned to detecting subtle abnormalities associated with HS. By the time we entered phase 2, agreement among the observers had increased substantially. Additionally, as image quality improved, subtle abnormalities were detected

**TABLE 2: Clinical and Imaging Findings in Temporal Lobectomy Patients in Whom Seizures Were Not Caused by Structural Lesions**

| Variable | Case No. | | | | | | | | | | |
|---|---|---|---|---|---|---|---|---|---|---|---|
| | 1 | 2 | 3 | 4 | 5 | 6 | 7 | 8 | 9 | 10 | 11 |
| Clinical | | | | | | | | | | | |
| Hippocampal sclerosis | + | + | + | + | + | + | + | + | + | – | – |
| Infantile febrile seizures | + | + | + | – | – | + | + | + | + | – | – |
| Ictal depth EEG | L med TL | L med TL | R med TL | L med TL | L med TL | R & L med TL | R med/lat TL | L med/lat TL | Not done | R med/lat TL | Unlocalized |
| Ictal scalp EEG | Unlocalized | R TL | Unlocalized | R hemisphere | Unlocalized | R hemisphere | R hemisphere | L hemisphere | R TL | R TL | Unlocalized |
| Side of speech | L | L | L | L | L | L | L | L | L | L | L |
| Side of surgery | L | L | R | L | L | R | R | L | R | R | R |
| Outcome | Excellent | Good | Excellent | Excellent | Excellent | Excellent | Fair | Excellent | Excellent | Poor | Fair |
| MR of hippocampus | | | | | | | | | | | |
| Atrophy | | | | | | | | | | | |
| Observer 1 | + | – | – | + | – | +++ | – | +++ | +++ | – | – |
| Observer 2 | – | – | +++ | + | + | +++ | + | + | – | – | + |
| Phase 2 | +++ | – | +++ | +++ | +++ | +++ | +++ | +++ | +++ | – | – |
| Signal | | | | | | | | | | | |
| Long TR/short TE | – | – | – | + | – | – | – | -- | +++ | – | – |
| Long TR/long TE | +++ | – | +++ | +++ | + | +++ | + | +++ | +++ | – | – |
| MR asymmetry | | | | | | | | | | | |
| Temporal lobe | | | | | | | | | | | |
| Observer 1 | – | L+++ | – | L+ | – | R+ | L+ | L+ | R+ | – | L+ |
| Observer 2 | L+ | L+ | R+++ | L+ | L+ | R+ | L+ | L+ | – | – | – |
| Temporal horn | | | | | | | | | | | |
| Observer 1 | – | R+ | – | – | – | – | R+++ | L+ | R+ | – | – |
| Observer 2 | – | – | R+++ | – | – | – | R+++ | – | – | – | – |
| Collateral white matter | + | – | Motion | + | + | + | + | + | – | – | – |
| Other abnormalities | R choroidal fissure cyst | – | – | L TL arachnoid cyst | – | – | Dysgenesis, corpus callosum | – | – | – | – |
| CT findings | | | | | | | | | | | |
| Observer 1 | R TL lesion | – | – | Small L TL cyst | – | – | Dysgenesis, corpus callosum | – | – | Artifact | – |
| Observer 3 | R TL lesion | – | – | Cyst | – | – | Dysgenesis, corpus callosum | – | – | – | – |

Note.—L = left; R = right; med = medial; lat = lateral; TL = temporal lobe. Hippocampal sclerosis was defined pathologically as hippocampal neuronal loss of greater than 50%. Opposite Ictal Depth EEG, lat TL refers to lateral (neocortical) temporal lobe foci. Multiple foci were found in cases 6 and 11, but predominant activity was from the right temporal lobe. The side of speech was localized by intracarotid artery Amytal test. The side of surgery refers to the side of anterior temporal lobectomy and radical hippocampectomy. It was also the side of pathologically proved hippocampal sclerosis. The diagnosis in cases 10 and 11 was nonspecific gliosis or atypical cryptogenic temporal lobe epilepsy (minimal hippocampal neuronal loss). Outcome was judged on the basis of the success of surgical treatment for epilepsy based on the decrease in the number of seizures with a 2- to 4-year follow-up: excellent = 100% decrease (rare seizures), good = >85% decrease, fair = >75% decrease, poor = <75% decrease. Hippocampal atrophy was graded as + (subtle or questionable atrophy), +++ (definite atrophy), or – (no atrophy). Atrophy was always seen ipsilateral to the side of surgery and pathologically proved hippocampal sclerosis. Signal within the hippocampus was graded as + (subtle or questionable hyperintensity), +++ (definite hyperintensity), or – (no hyperintensity). Temporal lobe and temporal horn asymmetry on MR were assessed relative to their presence (+) or absence (–) and the side of the smaller temporal lobe or the larger temporal horn: L+ = subtle or questionable left abnormality, L+++ = definite left abnormality, R+ = subtle or questionable right abnormality, R+++ = definite right abnormality. Angiography was unhelpful in all cases.

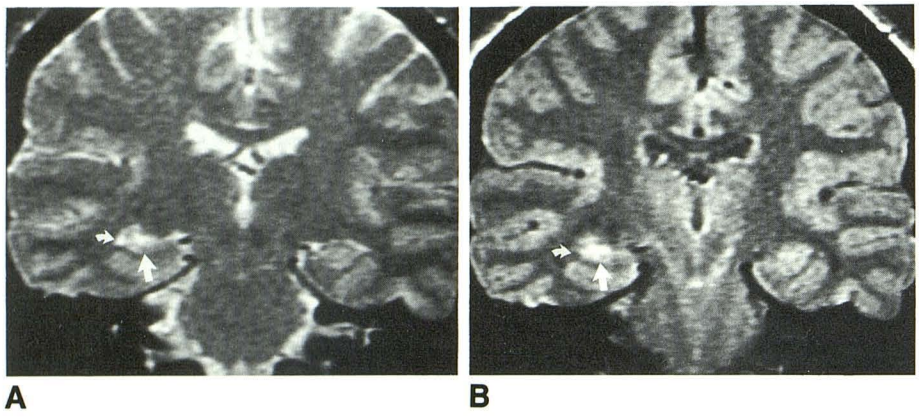


Fig. 4.—Right hippocampal sclerosis (case 9).

*A*, Coronal T2-weighted MR image at level of red nucleus. Hyperintense, flattened, atrophic right hippocampus (*straight arrow*) is contrasted with normal oval-shaped left hippocampus. Temporal horn (*curved arrow*).

*B*, Proton-density-weighted image. Hyperintense signal (*straight arrow*) on first-echo image confirms that this appearance is due to abnormal hippocampus and not adjacent CSF. Contrast this to hypointense signal from CSF in ventricle and temporal horn (*curved arrow*).

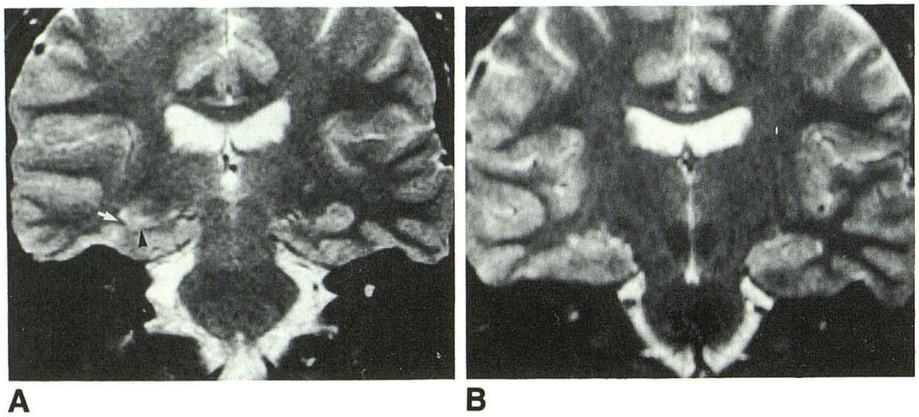


Fig. 5.—Right hippocampal sclerosis (case 6).

*A*, Coronal T2-weighted MR image at level of superior colliculus. Right hippocampal tail is atrophic and hyperintense (*arrowhead*). Adjacent collateral white matter (*arrow*) is also atrophic. Left side is normal.

*B*, At level of red nucleus. Collateral white matter on right side is not seen at this level. This leads to obscuration of borders between atrophic right hippocampus and adjacent neocortex.

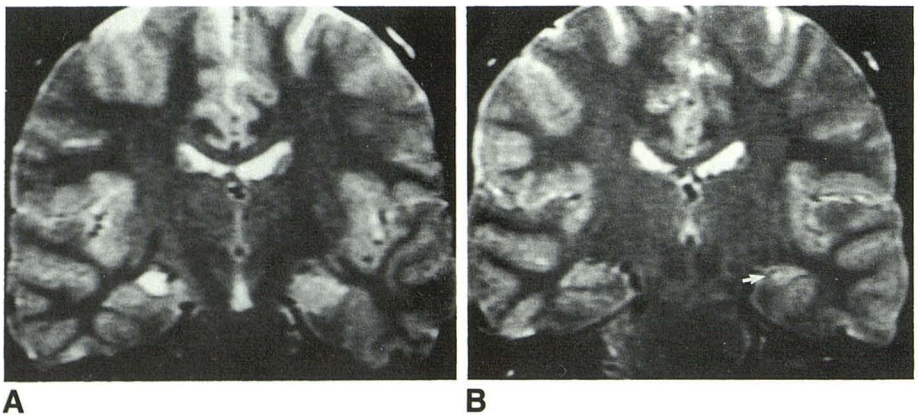


Fig. 6.—Left hippocampal sclerosis (case 1).

*A*, Coronal T2-weighted image at level of interpeduncular cistern. Incidental 1-cm cyst in right choroidal fissure is contralateral to clinical seizure focus and hippocampal sclerosis. During epilepsy evaluation, this was a source of confusion on axial CT, since a glioma was a diagnostic possibility. MR indicated this was a cyst in choroidal fissure. Owing to minimal head rotation, left hippocampus is imaged at level of head, while right is imaged at junction of head with body. This accounts for apparent enlargement of left hippocampus on this image and also emphasizes why it is easier to compare these structures at the body, a region where shape is more uniform.

*B*, MR image at level of red nucleus is able to visualize correct abnormality contralateral to cyst. Atrophic triangular left hippocampus is found on a slice 7.5 mm posterior to *A*. Focal region of hyperintensity within hippocampus is separated from CSF of choroidal fissure by fimbria (*arrow*) and alveus. There is subtle decrease in collateral white matter on left compared with right, which is considered pathologic in view of adjacent findings.

more easily and confidently. For example, the decreased interslice gap and smaller FOV used for the T1-weighted coronal images were helpful for confirming findings on T2-weighted sequences. Computer quantitation of the hippocampus appears to be accurate for lateralizing cryptogenic TLE and probably will play an important role in the future [18, 23].

Five of 20 non-HS epileptics also had hippocampal asymmetry. The hippocampus in normal people is rarely seen as atrophic [31]. Kim et al. [25] reported depletion in hippocampal neuronal density in patients with ipsilateral temporal lobe

**TABLE 3: Regional Atrophy in Patients with Hippocampal Sclerosis**

| Location | No. of Patients |
|---|---|
| Slice landmark | |
| Anterior pituitary | 0 |
| Posterior pituitary | 0 |
| Suprasellar cistern | 0 |
| Basilar artery | 4 |
| Interpeduncular cistern | 5 |
| Red nucleus | 7 |
| Posterior to red nucleus | 4 |
| Superior colliculus | 5 |
| Inferior colliculus | 0 |
| Posterior to colliculi | 0 |
| Limbic segment | |
| Amygdala | 1 |
| Head of hippocampus | 5 |
| Body of hippocampus | 8 |
| Tail of hippocampus | 5 |

Note.—Regional signal hyperintensity observed in hippocampal sclerosis usually paralleled regional atrophic changes.

**TABLE 4: Correlation of MR Measurements and Neuronal Density of Hippocampal Cell Regions**

| MR Measurement | Correlation Coefficient (r) by Hippocampal Cell Region | | | | |
|---|---|---|---|---|---|
| | CA1 | CA2 | CA3 | CA4 | Granule Cell |
| Height | NS | NS | .7403 ($p < .04$) | .6591 ($p < .03$) | .6014 ($p = .05$) |
| Width | NS | NS | .7342 ($p < .04$) | NS | .6271 ($p < .04$) |
| Product | NS | NS | .7645 ($p < .03$) | .6698 ($p < .03$) | .6882 ($p < .02$) |
| Ratio height[a] | NS | NS | NS | NS | NS |
| Ratio width[a] | NS | NS | NS | NS | .6028 ($p < .05$) |
| Ratio product[a] | NS | NS | NS | NS | NS |

Note.—CA = cornu ammonis; NS = not significant.
[a] Ratio refers to hippocampus on surgical side/hippocampus on nonsurgical side.

tumors as well as in HS. The neuronal decrease is not as marked in these patients as in patients with HS. We may be observing the MR correlate of these findings.

Most reports have used the abnormal signal within the medial temporal lobe as their major criterion for identifying HS. The abnormal signal is seen in the medial temporal lobe in 0–65% of patients with HS [12–15, 17, 18]. Kuzniecky et al. [13] postulate that the signal abnormality is due to gliosis and/or edema. In our patients, the hippocampal signal changes paralleled the atrophic changes, with the hippocampal body as the region most affected. The hyperintensity was always confined to the hippocampal formation in our patients (i.e., there was no extension outside the boundaries of the hippocampal formation). The alveus and fimbria separate the hyperintensity of the CSF above from the abnormal hippocampus below (Fig. 6). These findings are important in distinguishing tumors from HS. An abnormal signal confined to a small shrunken hippocampus was never seen with tumors.

Other imaging findings are less reliable for detecting HS, as demonstrated in this and other studies. These include ipsilateral atrophy of the temporal lobe and ipsilateral dilatation of the temporal horn [12–14, 18]. CT and angiography are even poorer methods for detecting HS [12, 13, 15, 16, 32, 33]. However, the use of multiple MR criteria can increase the level of suspicion for HS [12]. Our data indicate that collateral white matter atrophy may be an additional criterion (Fig. 5). Collateral white matter atrophy may be the MR correlate of sclerosis that extends beyond the hippocampal gray matter pathologically [19]. Signs of HS should be sought in all TLE patients since unrelated abnormalities can occur concurrently (Table 2, Fig. 6).

In view of the importance of diagnosing HS preoperatively (since its presence as evidenced by severe neuronal loss appears to determine the surgical outcome), we embarked on phase 3 of the present study. A strong correlation was found between the size of the hippocampus on MR at the plane of the red nucleus and neuronal cell density. The most striking correlation occurred in the comparison of product (height × width) on MR with neuronal densities in the CA3 and CA4 fields of the cornu ammonis and the granular cell layer (of the dentate gyrus). The most optimal MR measurements would have been cross-sectional area (and volumes) rather than a gross estimate derived from the product of height × width. We were seeking, however, a readily available method to assess the hippocampus on MR. In a separate study with a different group of patients, this issue was addressed by using computer-derived cross-sectional areas and volumes [23].

We might have expected some correlation with the CA1 region (the Sommer sector). Although neuronal depletion characteristic of HS frequently occurs in CA3 and CA4, cell loss in CA1 has been reported more frequently and to a greater degree [5, 25, 34]. Lencz et al. [23] found correlations between the degree of MR hippocampal asymmetry and neuronal density in CA1, CA3, CA4, and the granular cell layer. Jack et al. [18] used quantitative measurement of the hippocampus to lateralize the epileptogenic focus, but did not have neuronal densities available for comparative studies [18].

Nonorthogonal coronal imaging perpendicular to the hippocampal axis would be the preferred technique for measurement of the hippocampus if all else was equal. Since the software for this technique was not available at the time of our studies, we corrected for the orthogonal technique. The corrections were on the order of less than 10%. A newer technique, spoiled gradient-echo volume acquisitions, allows better gray-white differentiation and smaller slice thickness than spin-echo sequences do. For these reasons, spoiled gradient-echo imaging, which is restricted to the orthogonal planes, has replaced oblique coronal spin-echo sequences for quantifying the hippocampi at our institution. The method of correcting for hippocampal angles less than 90° can be used with this imaging sequence as well.

Identification of HS preoperatively has important clinical significance. Surgery can abort seizures in 60–90% of patients with medically refractory epilepsy [9, 10]. Until recently, invasive EEG has been required for confirmation of the seizure focus preoperatively [11]. Invasive EEG is associated with a 2–5% complication rate, additional hospitalization, and increased financial costs [11, 35]. If MR findings confirm localization of the seizure focus obtained by clinical, scalp EEG, and neurophsychological means, then depth electrodes may not be necessary before surgery [11].

REFERENCES


1. Spencer DD. Postscript: Should there be a surgical treatment of choice, and if so, how should it be determined. In: Engel J Jr, ed. *Surgical treatment of epilepsies.* New York: Raven, **1987**:477–484
2. Falconer MA, Serafetinides EA. A follow-up study of surgery in temporal lobe epilepsy. *J Neurol Neurosurg Psychiatry* **1963**;26:154–165
3. Brown WJ, Babb TL. Neuropathological changes in the temporal lobe associated with complex partial seizures. In: Hopkins A, ed. *Epilepsy.* London: Chapman & Hall, **1987**:300–324
4. Bruton CJ. *The neuropathology of temporal lobe epilepsy.* Oxford: Oxford University Press, **1988**
5. Margerison JH, Corsellis JAN. Epilepsy and the temporal lobes. *Brain* **1966**;89:499–529
6. Sano K, Malamud N. Clinical significance of sclerosis of the cornu ammonis. *Arch Neurol Psychiatry* **1953**;70:40–53
7. Rasmussen TB. Surgical treatment of complex partial seizures: results, lessons, and problems. *Epilepsia* **1983**;24[suppl 1):S65–S76
8. Falconer MA. Mesial temporal (Ammon's horn) sclerosis as a common cause of epilepsy. Aetiology, treatment, and prevention. *Lancet* **1974**;2:767–770
9. Spencer SS. Surgical options for uncontrolled epilepsy. *Neurol Clin* **1986**;4:669–695
10. Jensen I. Temporal lobe surgery around the world: results, complications and mortality. *Acta Neurol Scand* **1975**;52:354–373
11. Spencer SS, Spencer DD, Schwartz SS. The treatment of epilepsy with surgery. *Merritt Putnman Q* **1988**;5:3–17
12. McLachlan RS, Nicholson RL, Black S, Carr T, Blume WT. Nuclear magnetic resonance imaging, a new approach to the investigation of refractory temporal lobe epilepsy. *Epilepsia* **1985**;26:555–562
13. Kuzniecky R, de la Sayette V, Etheir R, et al. Magnetic resonance imaging in temporal lobe epilepsy: pathologic correlations. *Ann Neurol* **1987**;22:341–347
14. Brooks BS, King DW, El Gammal T, et al. MR imaging in patients with intractable complex partial epileptic seizures. *AJNR* **1990**;11:93–99
15. Sperling MR, Wilson G, Engel J Jr, Babb TL, Phelps M, Bradley W. Magnetic resonance imaging in intractable partial epilepsy: correlative studies. *Ann Neurol* **1986**;20:57–62
16. Heinz ER, Heinz TR, Radtke R, et al. Efficacy of MR vs CT in epilepsy. *AJNR* **1988**;9:1123–1128, *AJR* **1989**;152:347–352
17. Triulzi F, Franceschi M, Fazio F, Del Maschio A. Nonrefractory temporal lobe epilepsy: 1.5T MR imaging. *Radiology* **1988**;166:181–185
18. Jack CR, Sharbough FW, Twomey CK, et al. Temporal lobe seizures: lateralization with MR volume measurements of the hippocampal formation. *Radiology* **1990**;175:423–429
19. Falconer MA, Serafetinides EA, Corsellis JAN. Etiology and pathogenesis of temporal lobe epilepsy. *Arch Neurol* **1964**;10:233–248
20. Davidson S, Falconer MA. Outcome of surgery in 40 children with temporal-lobe epilepsy. *Lancet* **1975**;1:1260–1263
21. Duncan JS, Sagar HJ. Seizure characteristics, pathology, and outcome after temporal lobectomy. *Neurology* **1987**;37:405–409
22. De Lanerolle NC, Spencer DD. Neurotransmitter markers in human seizure foci. In: *Neurotransmitters and epilepsy: frontiers of clinical neurosciences.* Fisher RS, Coyle JT, eds. New York: Liss, **1990**:205–221
23. Lencz T, McCarthy G, Bronen R, Inserni J, Kim JH, Spencer DD. The hippocampus in temporal lobe epilepsy: correlation of pre-surgical MRI volumetrics with post-surgical cell counts. *Epilepsia* **1990**;31:667–668
24. Jack CR, Gehring DG, Sharbrough FW, et al. Temporal lobe volume measurements from MR images: accuracy and left-right asymmetry in normal persons. *J Comput Assist Tomogr* **1988**;12:21–29
25. Kim JH, Guimaraes PO, Shen MY, Masukawa LM, Spencer DD. Hippocampal neuronal density in temporal lobe epilepsy with and without gliomas. *Acta Neuropathol* (Berl) **1990**;80:41–45
26. Seab JP, Jagust WJ, Wong STS, Roos MS, Reed BR, Budinger TF. Quantitative NMR measurements of hippocampal atrophy in Alzheimer's disease. *Magn Reson Med* **1988**;8:200–208
27. Spencer DD, Spencer SS, Mattson RH, Williamson PD, Novelly RA. Access to the posterior medial temporal lobe structures in the surgical treatment of temporal lobe epilepsy. *Neurosurgery* **1984**;15:667–671
28. Jack CR, Twomey CK, Zinsmeister AR, Sharbrough FW, Petersen RC, Cascino GD. Anterior temporal lobes and hippocampal formations: normative volumetric measurements from MR images in young adults. *Radiology* **1989**;172:549–554
29. De Lanerolle NC, Kim JH, Robbins RJ, Spencer DD. Hippocampal interneuron loss and plasticity in human temporal lobe epilepsy. *Brain Res* **1989**;495:387–395
30. Kim JH, Guimaraes PO, Shen MY, Deutch C, Spencer SS, Spencer DD. Hippocampal volumetric neuronal density in temporal lobe epilepsy. In: *Society for Neuroscience Abstracts,* vol. 14. Washington, DC: Society for Neuroscience, **1988**:1032
31. Bronen RA, Cheung G. MRI of the normal hippocampus. *Magn Reson Imaging* **1991**;9:497–500
32. Jabbari B, Di Chiro G, McCarty JP. Mesial temporal sclerosis detected by computed tomography. *J Comput Assist Tomogr* **1979**;3:527–529
33. Blom RJ, Vinuela F, Fox AJ, Blume WT, Girvin J, Kaufmann JCE. Computed tomography in temporal lobe epilepsy. *J Comput Assist Tomogr* **1984**;8:401–405
34. Mouritzen Dam AM. Epilepsy in neuronal loss in the hippocampus. *Epilepsia* **1980**;21:617–629
35. Spencer DD. Depth electrode implantation at Yale University. In: Engle J Jr, ed. *Surgical treatment of the epilepsies.* New York: Raven **1987**: 603–607


The reader's attention is directed to the commentary on this article, which appears on pages 948–949.